

## Biochemical and Structural Analysis of the Interaction between $\beta$ -Amyloid and Fibrinogen

### Short title: Analysis of the A $\beta$ -fibrinogen interaction

Authors: Daria Zamolodchikov<sup>1</sup>, Hanna E. Berk-Rauch<sup>1</sup>, Deena A. Oren<sup>2</sup>, Daniel S. Stor<sup>1</sup>, Pradeep K. Singh<sup>1</sup>, Masanori Kawasaki<sup>3</sup>, Kazuyoshi Aso<sup>3</sup>, Sidney Strickland<sup>1</sup>, Hyung Jin Ahn<sup>1</sup>

1. Patricia and John Rosenwald Laboratory of Neurobiology and Genetics, The Rockefeller University, New York, NY 10065, USA; 2. Structural Biology Resource Center, The Rockefeller University, New York, NY 10065, USA; 3. Tri-Institutional Therapeutics Discovery Institute, New York, NY 10021, USA

Contact: Hyung Jin Ahn Ph.D, Laboratory of Neurobiology and Genetics, The Rockefeller University; 1230 York Ave, New York, NY 10065; e-mail: [hahn@rockefeller.edu](mailto:hahn@rockefeller.edu).

Text word count: 3984

Abstract word count: 214

Figures: 6

References: 32

Scientific category: Thrombosis and Hemostasis

### KEY POINTS

1. Binding to fibrinogen is mediated by the central region of A $\beta$ 42 and is enhanced by its C-terminal residues
2. A $\beta$ 42 binds the  $\alpha$ C region of fibrinogen, delaying plasmin-mediated fibrin cleavage and generating a persistent  $\alpha$ C degradation product

## Abstract

The majority of patients with Alzheimer's disease (AD) suffer from impaired cerebral circulation. Accumulating evidence suggests that fibrinogen, the main protein component of blood clots, plays an important role in this circulatory dysfunction in AD. Fibrinogen interacts with  $\beta$ -amyloid ( $A\beta$ ), forming plasmin-resistant abnormal blood clots, and increased fibrin deposition is found in the brains of AD patients and mouse models. In this study, we investigated the biochemical and structural details of the  $A\beta$ -fibrinogen interaction. We identified the central region of  $A\beta_{42}$  as the most critical region for the interaction, which can be inhibited by specific antibodies against the central region of  $A\beta$  and by naturally occurring p3 peptides,  $A\beta_{17-40}$  and  $A\beta_{17-42}$ . X-ray crystallographic analysis revealed that  $A\beta_{42}$  binding to fragment D of fibrinogen induced a structural change in the C-terminal region of the fibrinogen  $\beta$ -chain ( $\beta_{384-393}$ ). Furthermore, we identified an additional  $A\beta$  binding site within the  $\alpha C$  region of fibrinogen.  $A\beta$  binding to this  $\alpha C$  region blocked plasmin-mediated fibrin cleavage at this site, resulting in the generation of increased levels of a plasmin-resistant fibrin degradation fragment. Overall, our study elucidates the  $A\beta$ -fibrinogen interaction and clarifies the mechanism by which  $A\beta$ -fibrinogen binding delays fibrinolysis by plasmin. These results may facilitate the development of effective therapeutics against the  $A\beta$ -fibrinogen interaction to treat cerebrovascular abnormalities in AD.

## INTRODUCTION

Accumulating evidence implicates fibrin(ogen), the main protein component of blood clots, in Alzheimer's disease (AD) pathogenesis<sup>1-3</sup>. Activation of the coagulation cascade results in the cleavage of soluble fibrinogen to fibrin, which polymerizes to form an insoluble network. Since fibrin is occlusive<sup>4</sup> and proinflammatory<sup>5</sup>, its clearance (fibrinolysis) by plasmin is a tightly regulated process. Disturbances to fibrinolysis may therefore have significant consequences for

occlusive and inflammatory pathology in various diseases, including AD. Indeed, increased fibrin accumulation in the brains of AD patients and mouse models is correlated with areas of neuronal dysfunction<sup>6</sup>.

We have previously identified the AD-related peptide,  $\beta$ -amyloid ( $A\beta$ ), as a factor capable of modulating fibrin clot structure and stability<sup>7, 8</sup>.  $A\beta_{42}$  binds fibrinogen with a  $K_d$  of  $26.3 \pm 6.7\text{nM}$ <sup>7</sup>, and fibrin clots formed in the presence of  $A\beta_{42}$  are structurally altered and more resistant to fibrinolysis.  $A\beta_{42}$  can also bind to pre-formed fibrin and block the access of plasmin to fibrin<sup>8</sup>. Fibrinogen, which is composed of two fragment D domains and one fragment E domain, is a heterodimer composed of pairs of  $\alpha$ ,  $\beta$ , and  $\gamma$  chains<sup>9</sup>.  $A\beta_{42}$  binds  $\beta$ -chain residues  $\beta_{366-414}$  within fragment D<sup>7</sup>. This region is in close proximity to the b-hole of fibrinogen<sup>10</sup>, which is involved in the lateral aggregation of fibrin protofibrils<sup>11, 12</sup>.

Two different types of therapeutics targeting  $A\beta$ -fibrinogen association have been investigated<sup>2, 13</sup>. The root extract of *Aristolochia indica* efficiently degrades fibrin- $A\beta$  co-aggregates *in vitro* and in a rat model<sup>13</sup>. Furthermore, long-term treatment with RU-505, a specific inhibitor of the  $A\beta$ -fibrinogen interaction, results in reduced thrombosis, decreased AD pathology, and improved cognitive performance in a mouse model of AD<sup>2</sup>. Although both novel therapeutics targeting the  $A\beta$ -fibrinogen interaction in AD are effective *in vitro* and *in vivo*, low selectivity of the enzyme from *Aristolochia indica* and micro-molar  $IC_{50}$  levels of RU-505 limit their capabilities for clinical development. To improve selectivity and potency of therapeutics against the  $A\beta$ -fibrinogen interaction, a better understanding of the  $A\beta$ -fibrinogen interaction is needed.

Here, we analyzed the region within A $\beta$  responsible for A $\beta$ -fibrinogen binding using biochemical approaches and examined the structural aspects of binding between A $\beta$  and fragment D of fibrinogen using X-ray crystallography. In addition, we further investigated the mechanism by which A $\beta$ -fibrinogen binding delays fibrinolysis by plasmin.

## METHODS

### Preparation of A $\beta$ 42 and fibrinogen fragment D

A $\beta$ 42 (Anaspec) was reconstituted in a minimal volume of 0.1% NH<sub>4</sub>OH and then diluted to desired concentration with 50mM Tris or phosphate-buffered saline (pH 7.4). Solubilized A $\beta$ 42 was spun at 12,000 x g for 15 min to remove aggregated material<sup>14</sup> and the concentration was established by BCA (Thermo Scientific). Fibrinogen fragment D was prepared and purified as previously described<sup>15</sup>.

### Identification of fibrinogen-binding domains on A $\beta$

***Fibrinogen or fragment D binding assay using biotinylated A $\beta$  fragments.*** Synthetic N-terminally biotinylated A $\beta$  fragments 1-16, 15-25, 22-41, and 1-42 (50nM, Anaspec) were incubated with fibrinogen (5nM, Calbiochem) or fragment D (100nM) for 1 hr at RT in 50mM Tris pH7.4 containing 500mM NaCl, 0.01% BSA, protease inhibitor cocktail (Roche), and 0.01% NP-40 or 0.05% Tween-20. Streptavidin coated magnetic beads (Dynabeads M-280, Thermo-Fisher) were added for 30 min, washed, and eluted with non-reducing 1x LDS sample buffer (Thermo Fisher Scientific). Eluates were analyzed by SDS-PAGE on a 4-20% Tris-glycine gradient gel (Life Sciences) followed by Western blot using a polyclonal antibody against fibrinogen (Dako). For the AlphaLISA assay, various concentrations (0.02 - 20 $\mu$ M) of N-

terminally biotinylated A $\beta$  fragments 1-16, 15-25, 22-41, and 1-42 (50nM, Anaspec) were incubated with 1nM fibrinogen for 30 min at RT in final volume of 10  $\mu$ l assay buffer (25mM Tris-HCl, pH 7.4, 150mM NaCl, 0.05% Tween-20, 0.1% BSA) in white 384-well plates (Greiner). The mixture was incubated with the anti-fibrinogen antibody, 20 $\mu$ g/ml streptavidin-conjugated donor, and protein A-conjugated acceptor beads (Perkin-Elmer) for 90 min at RT. Samples were read by a PerkinElmer EnVision plate reader.

***A $\beta$ -fibrinogen interaction inhibition assay using non-biotinylated A $\beta$  fragments.*** Various concentrations (0.05 - 20 $\mu$ M) of 16 non-biotinylated A $\beta$  fragments listed in Supplemental Figure 1 (Anaspec or rPeptide) were plated in white 384-well plates and incubated with 10nM biotinylated A $\beta$ 42 and 1nM fibrinogen for 30 min at RT. The rest of the AlphaLISA assay was performed as described above, and the data fitted to a sigmoidal dose-response equation ( $Y = \text{Bottom} + (\text{Top} - \text{Bottom}) / (1 + 10^{(\log IC_{50} - X) \cdot \text{Hill coefficient}})$ ) using GraphPad Prism 4 to calculate half-maximal inhibition (IC<sub>50</sub>). For pull-down experiments, various concentrations of non-biotinylated A $\beta$ 17-42 were incubated with fragment D (200nM) and biotinylated A $\beta$ 42 (50nM) for 30 min. The rest of pull-down assay was performed as described above.

Five alanine scanning peptides, L17A, V18A, F19A, F20A, and D23A, were synthesized by replacing L17, V18, F19, F20, or D23 in A $\beta$ 17-42 with alanine (Chinese Peptide Company). Various concentrations (0.01 - 20 $\mu$ M) of alanine-scanning A $\beta$ 17-42 peptides were incubated with 10nM biotinylated A $\beta$ 42 and 1nM fibrinogen for 30 min at RT. The rest of the AlphaLISA assay was performed as described above.

***A $\beta$ -fibrinogen interaction inhibition assay using antibodies raised against specific regions of A $\beta$ .*** Biotinylated A $\beta$ 42 (50nM) and fibrinogen (5nM) were incubated with anti-A $\beta$  antibodies 3D6 (50nM; Elan), 6F/3D (50nM; Dako), 4G8 (50nM; Covance), ab62658 (50nM; Abcam), or G2-11 (50nM; Abcam) in 50mM Tris pH 7.4 containing 150mM NaCl, 0.01% NP-40,

0.01% BSA and protease inhibitor cocktail, and pull-down assays were performed as described above.

### **SDS-stable complex formation**

Fragment D (126  $\mu$ M) was incubated with A $\beta$ 42 or A $\beta$ 42 G37D (111  $\mu$ M) in 50mM Tris pH 7.6 with or without 1mM EDTA for 5 days at 37°C. Fibrinogen (14.7 $\mu$ M) was incubated with A $\beta$ 42 mutant G37D (30 $\mu$ M; Anaspec) in 50mM Tris pH 7.6 for 24 hours at 37°C. SDS-denaturation was carried out at 100 C° for 5 minutes under non-reducing conditions and samples were analyzed by Western blot using antibodies against A $\beta$  (6E10; Covance) and fibrinogen (Dako).

### **Crystallization of fibrinogen fragment D and of the fragment D-A $\beta$ 42 complex**

Fragment D crystals were obtained with the assistance of the Rockefeller University Structural Biology Resource Center as described in Everse et al.<sup>15</sup>. Briefly, crystals were obtained by sitting drop vapor diffusion at 4°C from 50mM Tris, pH 8.5, 70mM CaCl<sub>2</sub>, 2mM sodium azide, 12-17% polyethylene glycol (PEG) 3350 in drops of 10-20 $\mu$ l, with fragment D at 15mg/ml. A $\beta$ 42 or TAMRA (5-Carboxy-tetramethylrhodamine)-A $\beta$ 42 (Anaspec) were reconstituted to 0.7-1.5mg/ml in 50mM Tris, pH 8.5 with 0.1% NH<sub>4</sub>OH, then diluted 2-fold in 2X reservoir buffer (50mM Tris pH 8.5, 4mM sodium azide, 140mM CaCl<sub>2</sub>, 34% PEG 3,350) to yield A $\beta$  peptides in 1X reservoir buffer. Fragment D crystals were then soaked in the A $\beta$  solution (containing an excess of A $\beta$  over fragment D) at 4°C. Crystals soaked for 6 hours with TAMRA-A $\beta$ 42 were washed 3 times with reservoir buffer and imaged using a fluorescence microscope (Zeiss). Crystals soaked for 2 weeks with unlabeled A $\beta$ 42 were frozen in the N<sub>2</sub> cryostream in reservoir buffer without cryoprotection and diffracted to 3.3 Å at the National Synchrotron Light Source,

Brookhaven National Laboratory (Beam line X25, wavelength = 1.1Å). Data were also obtained to 2.9Å for crystals not subjected to soaking (native crystals). Data reduction was performed using HKL2000 software. Molecular replacement and subsequent refinement were performed with PHENIX software (PHENIX-dev-1555)<sup>16</sup> using the PDB entry 1FZA for fragment D<sup>17</sup>.

### **Analysis of A $\beta$ -induced delayed fibrinolysis**

The effect of A $\beta$  on fibrin degradation by plasmin was analyzed by an *in vitro* fibrin clot formation and degradation assay<sup>8</sup>. Briefly, fibrinogen (1.5 $\mu$ M) with or without A $\beta$ 42 (3 $\mu$ M) was mixed with plasminogen (250nM) in 20 mM HEPES buffer (pH 7.4) with 137mM NaCl. Fibrin clot formation and degradation were initiated by adding thrombin (0.5U/ml; Sigma), tPA (0.15nM; kindly provided by Genentech), and CaCl<sub>2</sub> (5mM) in a final volume of 150 $\mu$ l. Assays were performed at RT in 96-well plates (Fisher Scientific) in triplicate, and fibrin clot formation and degradation were monitored at 450nm using a Molecular Devices Spectramax Plus384 reader. Reactions were stopped after 8 hours by adding reducing 4x LDS sample buffer containing 100mM dithiothreitol (DTT). Fibrin degradation products were analyzed by SDS-PAGE on a 4-20% Tris-glycine gradient gel and visualized by Colloidal Blue Stain (Invitrogen).

**Mass spectrometric analysis of fibrin degradation products.** A protein gel band resistant to degradation in the presence of A $\beta$ 42 was excised and submitted to the Rockefeller University Proteomics Resource Center for mass spectrometric analysis (see Supplemental Methods).

**Edman sequencing of fibrin degradation products.** See Supplemental Methods.

**Identification of A $\beta$ 42-binding fibrinogen degradation products.** Fibrinogen (15 $\mu$ M in 50mM Tris, pH 8.0, 150mM NaCl, 5mM iodoacetamide) was incubated with 140nM plasminogen and 20nM tPA for 6 hours at 37°C to generate fibrinogen degradation products (FDPs).

Digestions were stopped with aprotinin (Sigma). FDPs (500 $\mu$ l) were incubated for 3 hours at RT with synthetic N-terminally biotinylated A $\beta$ 42 (2 $\mu$ M) in PBS adjusted to contain 500mM NaCl, 0.01% NP-40 and protease inhibitor cocktail, the A $\beta$ -interacting peptides pulled down with streptavidin-sepharose beads (Invitrogen) for 1 hours at RT, and the peptides eluted with sample loading buffer and analyzed by SDS-PAGE on a 4-20% Tris-glycine gradient gel. FDPs bound to biotin-labeled A $\beta$ 42 were visualized by Colloidal Blue Stain. Incubations that did not contain biotinylated A $\beta$ 42 served as a control for non-specific binding to the streptavidin-sepharose beads. Mass spectrometric analysis on bands pulled down by A $\beta$ 42 was performed by the Rockefeller University Proteomics Resource Center as described in Supplemental Methods.

## RESULTS

### Identification of the fibrinogen binding region within A $\beta$ 42.

To determine which region of A $\beta$ 42 is responsible for fibrinogen binding, three biotinylated A $\beta$  fragments (A $\beta$ 1-16, A $\beta$ 15-25 and A $\beta$ 22-41) were analyzed for their ability to bind fibrinogen and fragment D by pull-down assay. Among the three fragments, only A $\beta$ 22-41 showed binding to both fibrinogen (Figure 1A) and fragment D (Figure 1B). We next analyzed the binding affinity of these fragments to fibrinogen (Figure 1C) and fragment D (Figure 1D) using AlphaLISA. A $\beta$ 42 and A $\beta$ 22-41 dose-dependently bound to fibrinogen and fragment D (Figure 1C & 1D), while A $\beta$ 1-16 or A $\beta$ 15-25 showed no binding.

While the binding affinity of A $\beta$ 22-41 to Fragment D was more than 50% of A $\beta$ 42 (Figure 1B & 1D), the binding affinity of A $\beta$ 22-41 to fibrinogen was only 10-20% of A $\beta$ 42 (Figure 1A & 1C), indicating that an additional A $\beta$ 42 region may be involved in A $\beta$ 42-fibrinogen binding. These results also suggest that there are additional A $\beta$ 42 binding sites on fibrinogen outside of

fragment D and that the decrease in binding affinity of A $\beta$ 22-41 to fibrinogen may be due to a loss of affinity of A $\beta$ 22-41 for those binding sites. Overall, both the pull-down and AlphaLISA results indicate that the C-terminal two thirds of A $\beta$  are involved in binding fibrinogen and fragment D.

We further narrowed down the fibrinogen-binding region within A $\beta$ 42 using 16 non-biotinylated A $\beta$  peptide fragments spanning the entire length of A $\beta$ 42 (Supplemental Figure 1). Of the 16 A $\beta$  fragments, only A $\beta$ 17-40 and A $\beta$ 17-42 inhibited A $\beta$ -fibrinogen binding by AlphaLISA (Figure 2A), with A $\beta$ 17-42 having 10-fold higher inhibitory efficacy ( $IC_{50} = 1.03 \mu M$ ) compared to A $\beta$ 17-40 ( $IC_{50} = 13.4 \mu M$ ). All other A $\beta$  fragments, including A $\beta$ 1-17 and A $\beta$ 12-28, had no inhibitory activity (Figure 2A), and a combination of A $\beta$ 1-16 and A $\beta$ 17-42 did not have a higher inhibitory effect than A $\beta$ 17-42 alone (Supplemental Figure 2). The inhibitory efficacy of A $\beta$ 17-42 was confirmed via pull-down assay, where pull-down of fragment D by biotinylated A $\beta$ 42 was dose-dependently decreased in the presence of non-biotinylated A $\beta$ 17-42 (Figure 2B). Our AlphaLISA and pull-down results indicate that A $\beta$ 17-40 and A $\beta$ 17-42, naturally occurring A $\beta$  fragments known as p3 peptides<sup>18</sup>, inhibit the A $\beta$ 42-fibrinogen interaction, suggesting that these peptides may play a physiological role in modulating A $\beta$ 42-mediated effects on fibrin clots.

To analyze which amino acids within A $\beta$ 17-42 are important for the A $\beta$ -fibrinogen interaction, we tested the ability of five alanine-scanning peptide analogs of A $\beta$ 17-42, where L<sup>17</sup>, V<sup>18</sup>, F<sup>19</sup>, F<sup>20</sup>, or D<sup>23</sup> were replaced with alanine (L17A, V18A, F19A, F20A, and D23A), to inhibit A $\beta$ 42-fibrinogen binding by AlphaLISA. Analog peptides L17A and D23A exhibited almost no inhibitory activity, while F19A and F20A showed comparable inhibitory efficacy to original A $\beta$ 17-42. Interestingly, A $\beta$  V18A ( $IC_{50} = 0.26 \mu M$ ) showed 5-fold higher inhibitory efficacy than A $\beta$ 17-42 (Figure 2C).

This alanine scanning experiment indicates that L17 and D23 are crucial for A $\beta$ -fibrinogen binding.

Fragments of A $\beta$ 42 may adopt a different tertiary structure compared to A $\beta$ 42, which may affect their ability to bind to fibrinogen. We therefore examined the ability of biotinylated A $\beta$ 42 to bind fibrinogen in the presence of antibodies raised against specific regions of A $\beta$  (Figure 3A). Antibody 6F/3D (against A $\beta$ 8-17) and 4G8 (against A $\beta$ 17-24) blocked pull-down of fibrinogen by biotinylated A $\beta$ 42 (Figure 3B), while antibodies raised against A $\beta$ 1-5, A $\beta$ 22-35, and A $\beta$ 33-42 had no effect on A $\beta$ 42-fibrinogen binding. The epitopes of antibodies 6F/3D and 4G8 were confirmed by ELISA, which showed that 6F/3D bound A $\beta$ 1-16 and 1-17 but not A $\beta$ 17-42, whereas 4G8 only bound A $\beta$ 17-42 (Supplemental Figure 3). Thus, the central region of tertiary structured A $\beta$ 42 is critical for the A $\beta$ -fibrinogen interaction.

### **SDS-stable A $\beta$ -fibrinogen complex formation**

Our analysis of the A $\beta$ -fibrinogen interaction suggested that prolonged incubation of A $\beta$  and fragment D resulted in the formation of an SDS-stable complex. Since A $\beta$ 42 aggregates rapidly, we first examined this phenomenon using A $\beta$ 42 mutant G37D, which does not readily aggregate<sup>19</sup>. Prolonged incubation of fragment D with A $\beta$  G37D followed by Western blot analysis with an anti-A $\beta$  antibody showed A $\beta$ 42 G37D migrating at ~4.5kDa (corresponding to monomeric A $\beta$ ) as well as at ~100kDa (Figure 4A). The ~100 kDa band was not detected in the A $\beta$ 42 G37D alone lane, indicating that it is a specific product of A $\beta$ 42 G37D-fragment D interaction. Anti-fibrinogen antibodies detected fragment D at ~100 kDa, suggesting that the ~100kDa band detected by anti-A $\beta$  antibodies represents A $\beta$ 42 G37D that remained in complex with fragment D during SDS-PAGE. SDS-stable complex formation could be mediated by the

transglutaminase factor XIII (FXIII), which may contaminate fragment D preparations and lead to the formation of covalent crosslinks between A $\beta$  and fragment D. FXIII activity is dependent on calcium<sup>20</sup>, and incubation of fragment D with A $\beta$  G37D in the presence of EDTA, a calcium chelator, still resulted in SDS-stable complexes, indicating that FXIII-mediated crosslinking is not involved in SDS-stable complex formation.

SDS-stable complex formation was also observed when A $\beta$ 42 G37D was incubated with fibrinogen instead of fragment D (Figure 4B) and when A $\beta$ 42 was used instead of A $\beta$ 42 G37D (Figure 4A). Interestingly, incubation of non-mutant A $\beta$ 42 with fragment D resulted in the formation of fewer A $\beta$ 42 oligomers (~36-100 KDa) compared to when A $\beta$ 42 was incubated alone. Previous results show that the interaction between A $\beta$ 42 and fibrinogen or fragment D promotes A $\beta$ 42 fibrillization<sup>7</sup>, which could account for the conversion of the oligomeric species of A $\beta$ 42 seen when incubated alone into fibrils in the presence of fragment D.

### **A $\beta$ binding to fragment D induces structural change in C-terminal region of $\beta$ -chain**

Structural details of the A $\beta$ 42-fibrinogen interaction were investigated via X-ray crystallography. We sought to obtain a crystal structure of the A $\beta$ 42-fragment D complex because fragment D is the major binding region for A $\beta$  on fibrinogen, is smaller than fibrinogen, easier to manipulate, and has a published, reproducible crystal structure. Since large solvent channels are present in the fragment D structure, our strategy was to soak A $\beta$ 42 into pre-formed fragment D crystals. Fragment D crystals were obtained as described in Methods (Figure 5A). To test the ability of A $\beta$ 42 to penetrate into the crystal lattice, we soaked fragment D crystals with fluorescently labeled TAMRA (5-Carboxy-tetramethylrhodamine)-A $\beta$ 42 and non-specifically bound TAMRA-A $\beta$ 42 was removed by repeatedly washing the crystals until no decrease in fluorescence was observed. Persistent fluorescence visualized by fluorescence microscopy confirmed binding of

A $\beta$ 42 within the crystals (Figure 5B). Fragment D crystals were then soaked with unlabeled A $\beta$ 42, and data sets from soaked and unsoaked crystals were collected at the National Synchrotron Light Source. The structure was solved by molecular replacement as described in Methods. Soaking of A $\beta$ 42 did not damage fragment D crystals, since the space groups and unit cell dimensions obtained were mostly isomorphous with dimensions found in unsoaked (native) crystals, and agreed relatively well with published dimensions for fragment D (Figure 5C)<sup>15</sup>.

Analysis of electron density revealed that there were structural changes in A $\beta$ 42-soaked fragment D compared to data obtained from an unsoaked crystal. Specifically, a loop in the  $\beta$ -chain ( $\beta$ 384-393) of fragment D, which is a part of the A $\beta$ 42 binding region identified previously<sup>7</sup>, was shifted away from the coiled coil region when fragment D formed a complex with A $\beta$ 42 (Figure 5D). Fragment D structures crystallized in the presence of b-hole binding peptides (as in PDB 1FZG<sup>21</sup>, among others; Figure 5E) also showed that this loop is shifted in a similar but less dramatic way compared to the A $\beta$ 42-fragment D complex. Peptides binding the b-hole also induced a flip in a nearby loop ( $\beta$ 395-400), but this flip was not observed in our structure, suggesting that A $\beta$  may not fit all the way into the b-hole as the peptides do. Both A $\beta$ 42-soaked and unsoaked fragment D crystals were grown in identical conditions, and binding of A $\beta$ 42 within A $\beta$ 42-soaked crystals was confirmed using TAMRA-labeled A $\beta$ 42, suggesting that A $\beta$ 42 binding to fragment D induces the structural shift in the loop encompassing  $\beta$ 384-393.

We also observed patches of density unaccounted for by the fragment D coordinates possibly corresponding to A $\beta$ 42 in A $\beta$ 42-soaked but not unsoaked crystals. These patches of density were found in the region of fragment D in spatial proximity to the A $\beta$  binding site on the  $\beta$ -chain<sup>7</sup>, but the density was not sufficient to conclusively define A $\beta$ 42 placement (not shown). Based on the size of the water channels present in fragment D crystals and the size of the pocket near the  $\beta$ -chain region shown to bind A $\beta$ 42 ( $\beta$ 384-393)<sup>7</sup>, both A $\beta$ 42 monomers and dimers may enter

fragment D crystals during soaking. This non-homogeneous A $\beta$  population may have resulted in the indiscernible A $\beta$ 42 electron density map that we observed.

### **Binding of A $\beta$ to the fibrinogen $\alpha$ -chain blocks its cleavage by plasmin**

We previously found that A $\beta$ 42 binding to fibrin(ogen) interferes with plasmin(ogen) binding to fibrin and delays fibrin clot lysis<sup>1, 8</sup>. If A $\beta$ 42 binding to fibrin(ogen) interferes with plasmin(ogen)'s access to fibrin, then regions of fibrin(ogen) bound to A $\beta$ 42 would be expected to be protected from degradation. To investigate this idea, fibrin was formed in the presence and absence of A $\beta$ 42 and subjected to plasmin-mediated degradation. Analysis of the fibrin degradation products revealed a plasmin-resistant fibrin fragment (PRFF) migrating at ~ 20kDa (arrow in Figure 6A) that was observed only when fibrin was formed in the presence of A $\beta$ 42. Mass spectrometry analysis and N-terminal sequencing of the PRFF identified it as a fibrin  $\alpha$ -chain fragment that includes residues A $\alpha$ 239-421 (Figure 6B). Fibrin formed in the presence of A $\beta$ 42 is thinner, arranged in a denser network<sup>8</sup>, and interrupted by abnormal aggregates<sup>1</sup>. To control for the potentially confounding effects of this abnormal fibrin network on plasmin-mediated degradation, we performed the same experiment without thrombin. Fibrinogen incubated with A $\beta$ 42 and subjected to plasmin-mediated digestion also yielded the same degradation-resistant fragment (Figure 6A), indicating that PRFF formation is independent of changes to fibrin network structure induced by A $\beta$ 42.

To confirm that blockage of a plasmin cleavage site on the fibrin(ogen) A $\alpha$  chain by A $\beta$ 42 is involved in increased PRFF formation in the presence of A $\beta$ 42, we investigated whether A $\beta$ 42 can bind to this region of fibrinogen. Fibrinogen was partially digested with plasmin to generate large fibrinogen degradation products. Pull-down of the fibrinogen degradation products with biotinylated A $\beta$ 42 identified a fragment similar in size to the PRFF (arrow in Figure 6C). Mass

spectrometry analysis demonstrated that this fragment maps to the same region of the  $\alpha$ -chain as identified for the PRFF (Figure 6B). Together, these results suggest that A $\beta$ 42 binds to the  $\alpha$ -chain of fibrin(ogen) and blocks its cleavage by plasmin.

## DISCUSSION

We examined the fibrinogen-binding region within A $\beta$ 42 using four distinct biochemical approaches. The results from all four experimental approaches (summarized in Supplemental Figure 4) are closely aligned, but there is a slight difference between the results obtained using antibodies blocking specific regions of A $\beta$ 42 (Figure 3) and the approaches using A $\beta$  fragments. Competitive inhibition of the A $\beta$ -fibrinogen interaction using unlabeled A $\beta$  sub-peptides (Figure 2) showed that A $\beta$ 17-42 (IC<sub>50</sub> 1.03 $\mu$ M) had 10-fold higher inhibitory efficacy than A $\beta$ 17-40 (IC<sub>50</sub> 13.4 $\mu$ M). This supports our previous results showing that A $\beta$ 42 has a higher binding affinity to fibrinogen than A $\beta$ 40<sup>2</sup>, and suggests that the C-terminus of A $\beta$ 42 is important for its binding to fibrinogen. However, antibodies against the C-terminus of A $\beta$ 42 (G2-11; Figure 3) failed to block A $\beta$ 42-fibrinogen binding. One possible explanation for this difference is that while the C-terminus of A $\beta$ 42 may not be directly involved in the interaction between A $\beta$ 42 and fibrinogen, the two C-terminal residues of A $\beta$ 42 (Ile41 and Ala42) increase the stability of A $\beta$ 's tertiary structure and promote its oligomerization<sup>22, 23</sup>, which may enhance A $\beta$ -fibrinogen binding due to the fact that A $\beta$  oligomers have stronger binding affinity to fibrinogen than monomers<sup>2</sup>. It is therefore possible that once the tertiary structure and/or oligomeric state of A $\beta$ 42 are stabilized by its C-terminal residues, blocking the C-terminus using antibodies does not inhibit the A $\beta$ 42-fibrinogen interaction.

Overall, our results suggest that fibrinogen interacts with the central region of tertiary structured A $\beta$ 42, which is stabilized by its C-terminal residues. This binding model is similar to the interaction between ApoE3 and A $\beta$ 42, where binding is mediated by the central region of A $\beta$ 42 and further enhanced by its C-terminal residues<sup>24</sup>. By defining the binding regions on A $\beta$  and fibrinogen involved in their interaction, our results provide a basis for structure-based rational design of small molecule or antibody inhibitors targeting this interaction. Our results also suggest that targeting the tertiary stability of A $\beta$ 42 via its two C-terminal residues may be an alternative strategy for inhibiting A $\beta$ 42-fibrinogen binding.

We found that naturally occurring p3 peptides (A $\beta$ 17-40 and A $\beta$ 17-42) inhibit the A $\beta$ 42-fibrinogen interaction. The role of p3 peptides in AD pathogenesis is controversial. Some studies indicate that A $\beta$ 17-42 exhibits enhanced aggregation relative to full-length A $\beta$ 42<sup>25</sup> and that p3 peptides are prevalent in diffuse deposits and in a subset of dystrophic neurites in AD patients<sup>26</sup>. However, other studies suggest that p3 peptides might be a benign form of amyloid, since they lack domains associated with microglial activation<sup>27</sup>, do not form oligomers, which are the most toxic species of A $\beta$ <sup>18</sup>, and do not have negative effects on neuronal synaptic function<sup>28</sup>. Our present study demonstrates that p3 peptides compete with A $\beta$ 42 for binding to fibrinogen, suggesting that they may attenuate AD pathology. Therefore, the inhibition of the A $\beta$ 42-fibrinogen interaction by p3 peptides may be another beneficial consequence of enhancing alpha-secretase activity as a therapeutic strategy for AD<sup>29</sup>.

Prolonged incubation of A $\beta$ 42 with fibrinogen resulted in SDS-stable complex formation. Previously, A $\beta$ 42 has been shown to form SDS-stable complexes with ApoE2 and 3<sup>24</sup>. Since SDS-stable complex formation between A $\beta$  and its binding partners may impair protein function,

studies aimed at identifying the nature of the SDS-stable complexes involving A $\beta$  may shed light on new mechanisms by which A $\beta$  may contribute to pathological processes.

We have previously shown that A $\beta$ 42 binding to fibrin(ogen) delays fibrinolysis by interfering with the binding of plasminogen and plasmin to fibrin<sup>8</sup> and that A $\beta$ 42 binds to the  $\beta$ -chain of fibrinogen fragment D<sup>7</sup>. We also confirmed A $\beta$ 42-binding to fibrin D-dimer (Supplemental figure 5). The current study identifies an additional binding site for A $\beta$ 42 on the fibrin(ogen)  $\alpha$ C region, which is known to bind plasminogen and include several plasmin cleavage sites. A $\beta$ 42 binding to this  $\alpha$ C region results in the formation of a PRFF, likely via A $\beta$ 42-mediated interference with plasmin(ogen) binding to fibrin and with plasmin-mediated cleavage of fibrin at this site.

However, it is possible that A $\beta$ 42 binding to this region may inhibit other molecules that bind the  $\alpha$ C region of fibrin, such as tPA and  $\alpha$ 2-antiplasmin<sup>30-32</sup>. Investigating whether A $\beta$  binding to the fibrin(ogen)  $\alpha$ C region affects tPA and  $\alpha$ 2-antiplasmin binding to fibrin and whether there are functional consequences of these inhibitions would clarify the mechanism of PRFF formation. Furthermore, studies measuring the levels of PRFFs in the blood and brain parenchyma of individuals at various stages of disease would shed light on whether the PRFF could be useful as a biomarker for AD.

## **ACKNOWLEDGEMENTS**

This work was supported by the Alzheimer's Drug Discovery Foundation and Robertson Therapeutic Development Fund for HA; NIH grant NS50537; the Tri-Institutional Therapeutics Discovery Institute; the Alzheimer's Drug Discovery, Thome Memorial Medical, Litwin, Rudin Family, Blanchette Hooker Rockefeller, and Mellam Family Foundations; and John A. Herrmann, for SS. The Rockefeller University Structural Biology Resource Center is supported by grant

1S10RR022321-01 and 1S10RR027037-01 from the National Center for Research Resources, NIH. We thank the Rockefeller University High-Throughput and Spectroscopy Resource Center for access to experimental equipment and technical support. We thank N. Trikannad for experimental assistance, and M. Foley, E. Norris and Z. Chen for helpful discussion.

**Authorship contributions:** D.Z. and H.A. designed the study, performed experiments, analyzed data, and wrote the manuscript; H.E.B., P.K.S. and D.S.S. performed experiments and analyzed data; D.A.O. designed the structural study and assisted in experiments and data analysis; S.S. designed the study, participated in data analysis and manuscript preparation; M.K. and K.A., designed the study.

**Conflict-of-interest disclosure:** The authors declare no competing financial interests

## REFERENCES

1. Cortes-Canteli, M., J. Paul, E.H. Norris, R. Bronstein, H.J. Ahn, D. Zamolodchikov, S. Bhuvanendran, K.M. Fenz, and S. Strickland, Fibrinogen and beta-amyloid association alters thrombosis and fibrinolysis: a possible contributing factor to Alzheimer's disease. *Neuron*. 2010; 66 (5): 695-709.
2. Ahn, H.J., J.F. Glickman, K.L. Poon, D. Zamolodchikov, O.C. Jno-Charles, E.H. Norris, and S. Strickland, A novel Abeta-fibrinogen interaction inhibitor rescues altered thrombosis and cognitive decline in Alzheimer's disease mice. *J Exp Med*. 2014; 211 (6): 1049-62.
3. Narayan, P.J., S.L. Kim, C. Lill, S. Feng, R.L. Faull, M.A. Curtis, and M. Dragunow, Assessing fibrinogen extravasation into Alzheimer's disease brain using high-content screening of brain tissue microarrays. *J Neurosci Methods*. 2015; 247: 41-9.
4. Weisel, J.W. and R.I. Litvinov, Mechanisms of fibrin polymerization and clinical implications. *Blood*. 2013; 121 (10): 1712-9.

5. Davalos, D. and K. Akassoglou, Fibrinogen as a key regulator of inflammation in disease. *Semin Immunopathol.* 2012; 34 (1): 43-62.
6. Cortes-Canteli, M., L. Mattei, A.T. Richards, E.H. Norris, and S. Strickland, Fibrin deposited in the Alzheimer's disease brain promotes neuronal degeneration. *Neurobiol Aging.* 2015; 36 (2): 608-17.
7. Ahn, H.J., D. Zamolodchikov, M. Cortes-Canteli, E.H. Norris, J.F. Glickman, and S. Strickland, Alzheimer's disease peptide beta-amyloid interacts with fibrinogen and induces its oligomerization. *Proc Natl Acad Sci U S A.* 2010; 107 (50): 21812-7.
8. Zamolodchikov, D. and S. Strickland, Abeta delays fibrin clot lysis by altering fibrin structure and attenuating plasminogen binding to fibrin. *Blood.* 2012; 119 (14): 3342-51.
9. Weisel, J.W., Fibrinogen and fibrin. *Adv Protein Chem.* 2005; 70: 247-99.
10. Kostelansky, M.S., B. Bolliger-Stucki, L. Betts, O.V. Gorkun, and S.T. Lord, B beta Glu397 and B beta Asp398 but not B beta Asp432 are required for "B:b" interactions. *Biochemistry.* 2004; 43 (9): 2465-74.
11. Yang, Z., I. Mochalkin, and R.F. Doolittle, A model of fibrin formation based on crystal structures of fibrinogen and fibrin fragments complexed with synthetic peptides. *Proc Natl Acad Sci U S A.* 2000; 97 (26): 14156-61.
12. Lugovskoy, E.V., E.N. Zolotareva, G.K. Gogolinskaya, P.G. Gritsenko, E.D. Moroz, and S.V. Komisarenko, Polymerization sites in the D-domain of human fibrin(ogen). *Biochemistry (Mosc).* 2002; 67 (4): 446-50.
13. Bhattacharjee, P. and D. Bhattacharyya, An Enzyme from *Aristolochia indica* Destabilizes Fibrin-beta Amyloid Co-Aggregate: Implication in Cerebrovascular Diseases. *PLoS one.* 2015; 10 (11): e0141986.
14. Atwood, C.S., R.D. Moir, X. Huang, R.C. Scarpa, N.M. Bacarra, D.M. Romano, M.A. Hartshorn, R.E. Tanzi, and A.I. Bush, Dramatic aggregation of Alzheimer abeta by Cu(II) is induced by conditions representing physiological acidosis. *J Biol Chem.* 1998; 273 (21): 12817-26.
15. Everse, S.J., H. Pelletier, and R.F. Doolittle, Crystallization of fragment D from human fibrinogen. *Protein Sci.* 1995; 4 (5): 1013-6.
16. Adams, P.D., et al., PHENIX: a comprehensive Python-based system for macromolecular structure solution. *Acta Crystallogr D Biol Crystallogr.* 2010; 66 (Pt 2): 213-21.
17. Spraggon, G., S.J. Everse, and R.F. Doolittle, Crystal structures of fragment D from human fibrinogen and its crosslinked counterpart from fibrin. *Nature.* 1997; 389 (6650): 455-62.
18. Dulin, F., F. Leveille, J.B. Ortega, J.P. Mornon, A. Buisson, I. Callebaut, and N. Colloc'h, P3 peptide, a truncated form of A beta devoid of synaptotoxic effect, does not assemble into soluble oligomers. *FEBS Lett.* 2008; 582 (13): 1865-70.

19. Kanski, J., M. Aksenova, and D.A. Butterfield, The hydrophobic environment of Met35 of Alzheimer's Abeta(1-42) is important for the neurotoxic and oxidative properties of the peptide. *Neurotox Res.* 2002; 4 (3): 219-23.
20. Hornyak, T.J. and J.A. Shafer, Role of calcium ion in the generation of factor XIII activity. *Biochemistry.* 1991; 30 (25): 6175-82.
21. Everse, S.J., G. Spraggon, L. Veerapandian, and R.F. Doolittle, Conformational changes in fragments D and double-D from human fibrin(ogen) upon binding the peptide ligand Gly-His-Arg-Pro-amide. *Biochemistry.* 1999; 38 (10): 2941-6.
22. Olofsson, A., A.E. Sauer-Eriksson, and A. Ohman, The solvent protection of alzheimer amyloid-beta-(1-42) fibrils as determined by solution NMR spectroscopy. *J Biol Chem.* 2006; 281 (1): 477-83.
23. Evans, D.G., M. Ahmed, S. Bayliss, E. Howard, F. Laloo, and A. Wallace, BRCA1, BRCA2 and CHEK2 c.1100 delC mutations in patients with double primaries of the breasts and/or ovaries. *J Med Genet.* 2010; 47 (8): 561-6.
24. Munson, G.W., A.E. Roher, Y.M. Kuo, S.M. Gilligan, C.A. Reardon, G.S. Getz, and M.J. LaDu, SDS-stable complex formation between native apolipoprotein E3 and beta-amyloid peptides. *Biochemistry.* 2000; 39 (51): 16119-24.
25. Pike, C.J., M.J. Overman, and C.W. Cotman, Amino-terminal deletions enhance aggregation of beta-amyloid peptides in vitro. *J Biol Chem.* 1995; 270 (41): 23895-8.
26. Higgins, L.S., G.M. Murphy, Jr., L.S. Forno, R. Catalano, and B. Cordell, P3 beta-amyloid peptide has a unique and potentially pathogenic immunohistochemical profile in Alzheimer's disease brain. *Am J Pathol.* 1996; 149 (2): 585-96.
27. Dickson, D.W., The pathogenesis of senile plaques. *J Neuropathol Exp Neurol.* 1997; 56 (4): 321-39.
28. Walsh, D.M., I. Klyubin, J.V. Fadeeva, W.K. Cullen, R. Anwyl, M.S. Wolfe, M.J. Rowan, and D.J. Selkoe, Naturally secreted oligomers of amyloid beta protein potently inhibit hippocampal long-term potentiation in vivo. *Nature.* 2002; 416 (6880): 535-9.
29. Lichtenthaler, S.F., alpha-secretase in Alzheimer's disease: molecular identity, regulation and therapeutic potential. *J Neurochem.* 2011; 116 (1): 10-21.
30. Tsurupa, G. and L. Medved, Identification and characterization of novel tPA- and plasminogen-binding sites within fibrin(ogen) alpha C-domains. *Biochemistry.* 2001; 40 (3): 801-8.
31. Medved, L. and W. Nieuwenhuizen, Molecular mechanisms of initiation of fibrinolysis by fibrin. *Thromb Haemost.* 2003; 89 (3): 409-19.
32. Tsurupa, G., S. Yakovlev, P. McKee, and L. Medved, Noncovalent interaction of alpha(2)-antiplasmin with fibrin(ogen): localization of alpha(2)-antiplasmin-binding sites. *Biochemistry.* 2010; 49 (35): 7643-51.

## FIGURE LEGENDS

**Figure 1. A $\beta$ 22-41 binds to fibrinogen and fragment D.** (A & B) Biotin-labeled A $\beta$ 42, A $\beta$ 1-16, A $\beta$ 15-25, and A $\beta$ 22-41 were incubated with fibrinogen (FBG) or fragment D (FD), and pull-down assays were carried out using streptavidin-coated magnetic beads. All samples were analyzed by Western blot in unreduced condition using an anti-fibrinogen antibody. Only A $\beta$ 22-41 showed binding to both fibrinogen (A) and fragment D (B). When no A $\beta$  peptides were added, the level of bound fibrinogen or fragment D was negligible. Images and graphs are representative of 4 experiments. (C & D) The binding between biotin-labeled A $\beta$ 42 or A $\beta$  fragments with fibrinogen or fragment D was determined by AlphaLISA (n = 3). Controls and other lanes in figure 1A are from the same gel with some lanes omitted for clarity. Results presented in graphs are mean  $\pm$  SEM.

**Figure 2. Naturally occurring p3 peptides, A $\beta$ 17-40 and A $\beta$ 17-42, inhibit the A $\beta$ -fibrinogen interaction.** (A) Biotinylated A $\beta$ 42 was incubated with fibrinogen in the presence of various concentrations (0.05 - 20  $\mu$ M) of 16 non-biotinylated A $\beta$  fragments listed in Supplemental Figure 1. The inhibitory efficacy of the A $\beta$  fragments on the A $\beta$ 42-fibrinogen interaction was analyzed using AlphaLISA. Of the 16 A $\beta$  fragments tested, only A $\beta$ 17-40 (IC<sub>50</sub> = 13.4  $\mu$ M) and A $\beta$ 17-42 (IC<sub>50</sub> = 1.03  $\mu$ M) showed inhibitory efficacy (n = 3). (B) Western blot analysis with anti-fibrinogen antibody shows that A $\beta$ 17-42 blocks the ability of biotinylated A $\beta$ 42 to pull down fragment D (FD) in a dose-dependent manner. (C) Various concentrations (0.01 - 20  $\mu$ M) of five alanine scanning A $\beta$  peptides (L17A, V18A, F19A, F20A, and D23A) were incubated with biotinylated A $\beta$ 42 and fibrinogen, and their ability to inhibit the A $\beta$ 42-fibrinogen interaction was analyzed using AlphaLISA (n = 3 - 6). A $\beta$  L17A and D23A had almost no inhibitory activity (IC<sub>50</sub> > 20  $\mu$ M), while F19A (IC<sub>50</sub> = 3.7  $\mu$ M) and F20A (IC<sub>50</sub> = 6.8  $\mu$ M) showed a compatible inhibitory efficacy to original A $\beta$ 17-42. Interestingly, V18A (IC<sub>50</sub> = 0.26  $\mu$ M) had 5-fold greater inhibitory efficacy than A $\beta$ 17-42. Results presented in graphs are mean  $\pm$  SEM.

**Figure 3. Specific antibodies against the central region of A $\beta$  block the A $\beta$ -fibrinogen**

**interaction.** (A) The epitopes for several antibodies against A $\beta$  are illustrated in the schematic and include epitopes 1-5 (3D6, Elan), 8-17 (6F/3D, Dako), 17-24 (4G8, Covance), 22-35 (ab62658, Abcam), and 33-42 (G2-11, Abcam). (B) Antibodies at concentrations listed in Methods were incubated with fibrinogen and biotinylated A $\beta$ 42. Pull-down of biotinylated A $\beta$ 42 revealed that antibodies 6F/3D and 4G8 are able to interfere with the A $\beta$ -fibrinogen interaction. Results presented in graphs are mean  $\pm$  SEM, and statistical significance was determined using one-way ANOVA and Bonferroni post hoc test (\*\*,  $p < 0.01$ ;  $n = 3$ ).

**Figure 4. Long-term incubation of fibrinogen/fragment D with A $\beta$ 42 forms a SDS-stable**

**complex.** (A) A $\beta$ 42 G37D or A $\beta$ 42 was incubated with fragment D (FD) for 5 days at 37°C in the presence or absence of EDTA. Western blots were analyzed with antibody 6E10 against A $\beta$  (left panel) and an antibody against fibrinogen (Dako; right panel). A $\beta$ -fragment D SDS-stable complex was detected by 6E10. (B) A $\beta$ 42 G37D was incubated with fibrinogen (FBG) for 24 hours at 37°C. Western blots were analyzed with antibody 6E10 against A $\beta$  (left panel) and an antibody against fibrinogen (right panel). A $\beta$ -fibrinogen SDS-stable complex was also detected by 6E10 (arrow). Controls and other lanes in figure 4B are from the same gel with some lanes omitted for clarity.

**Figure 5. Fragment D structure is altered in the presence of A $\beta$ 42.** The fragment D crystals

soaked with A $\beta$ 42 were analyzed by X-ray crystallography. (A) Bright field (left) and UV fluorescence (right) images of fragment D crystals, indicating crystals are proteinaceous. (B) Left: Bright field image of a fragment D crystal that had been subjected to soaking in TAMRA-A $\beta$ 42 followed by extensive washing. Right: Persistent red fluorescence after washing indicated that TAMRA-A $\beta$ 42 was binding within the crystal. (C) Unit cell dimensions of published (1FZA), non-soaked, and A $\beta$ 42-soaked fragment D crystals. (D) Diagram of fibrinogen with fragment D (FD) marked by dashed box, and the location of altered structure in A $\beta$ 42-soaked fragment D

crystals indicated by solid pink lines. Superimposed 2Fo-Fc maps from non-soaked (yellow; R<sub>work</sub>/R<sub>free</sub> = 0.24/0.33) and A $\beta$ 42-soaked (teal; R<sub>work</sub>/R<sub>free</sub> = 0.28/0.39) fragment D crystals with coordinates of non-soaked crystals. (E) Protein backbone diagram showing the shift of the  $\beta$ 384-393 loop from non-soaked fragment D (pink) to b-hole peptide bound (1FZG; green) fragment D and A $\beta$ 42-soaked fragment D (blue).

**Figure 6. A $\beta$  interacts with the  $\alpha$ -chain of fibrinogen, producing a plasmin-resistant fibrin fragment during fibrinolysis.** (A) Fibrin was digested with plasmin in the presence or absence of A $\beta$ 42. A plasmin-resistant fragment was observed only in the presence of A $\beta$ 42 (arrow). The same experiment was done without thrombin. In the absence of thrombin, plasmin degradation-resistant PRFF was also observed in the presence of A $\beta$ 42. Images are representative of  $\geq 3$  experiments. (B) Mass spectrometry analysis of the fragments in (A) and (C) showed they were derived from the  $\alpha$ -chain of fibrinogen. Green residues were identified by N-terminal sequencing of band in (A), red residues were identified by mass spectrometry analysis of band in (A), and underlined residues were identified by mass spectrometry analysis of band in (C). (C) Fibrinogen was partially digested with plasmin, incubated with biotinylated A $\beta$ 42, and A $\beta$ 42 was pulled down with streptavidin (SA) coated beads. A fibrin fragment that bound to A $\beta$  was observed (top arrow).

# Figure 1

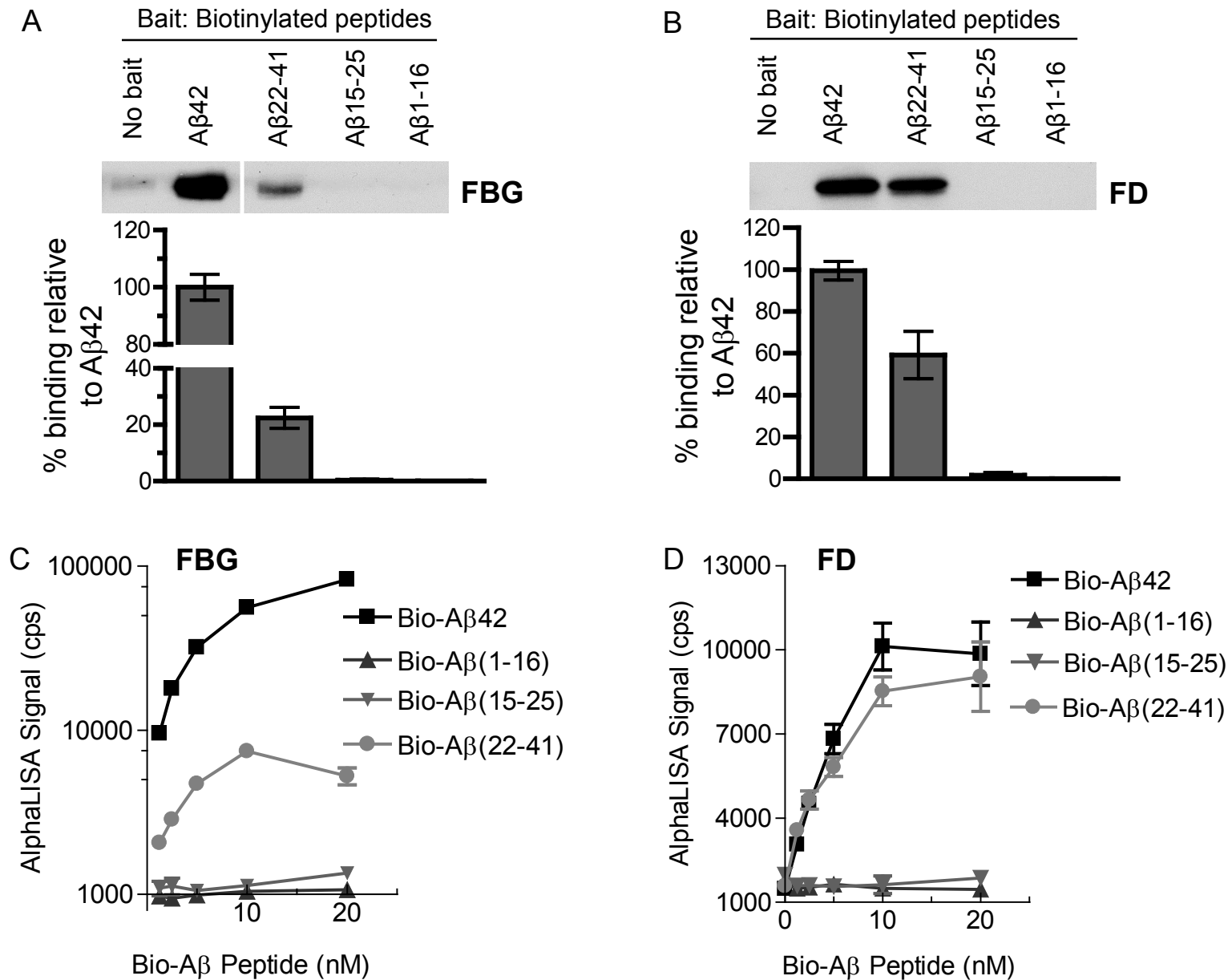


# Figure 2

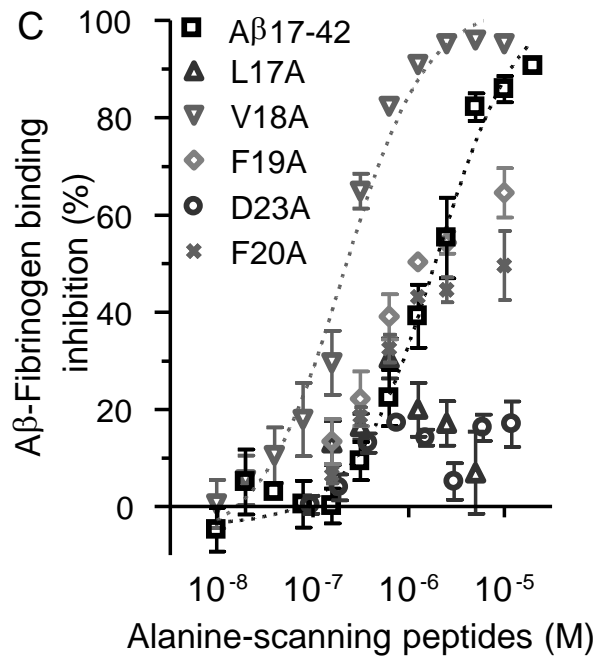
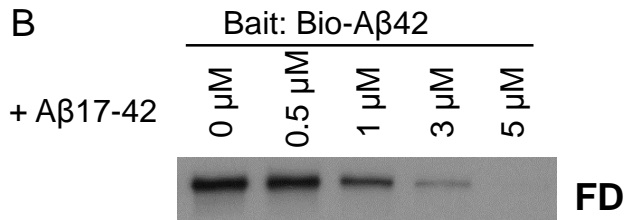
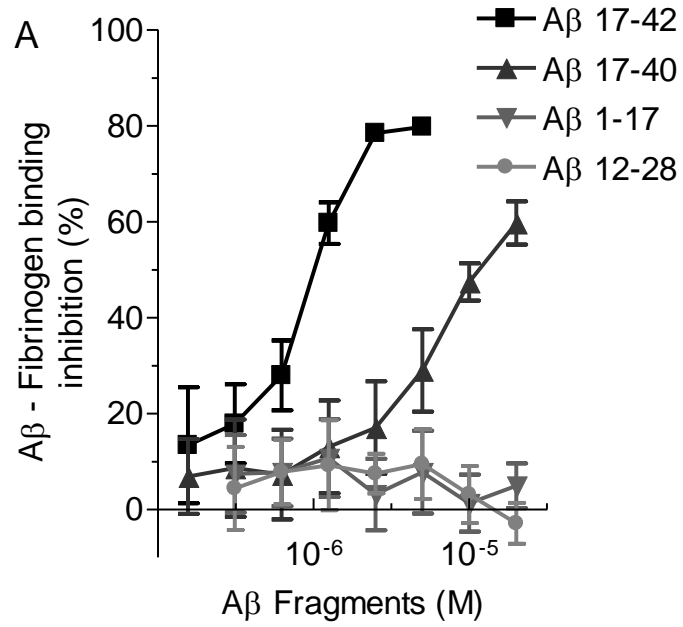


# Figure 3

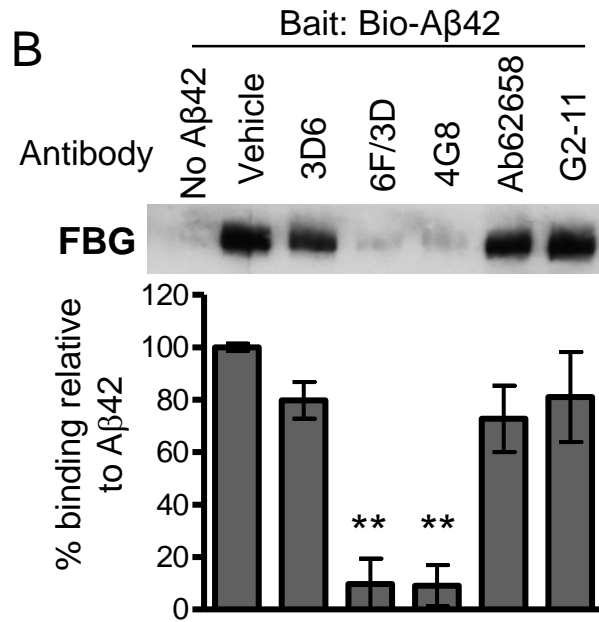
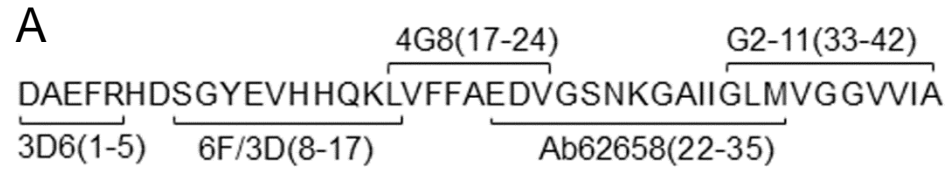


# Figure 4

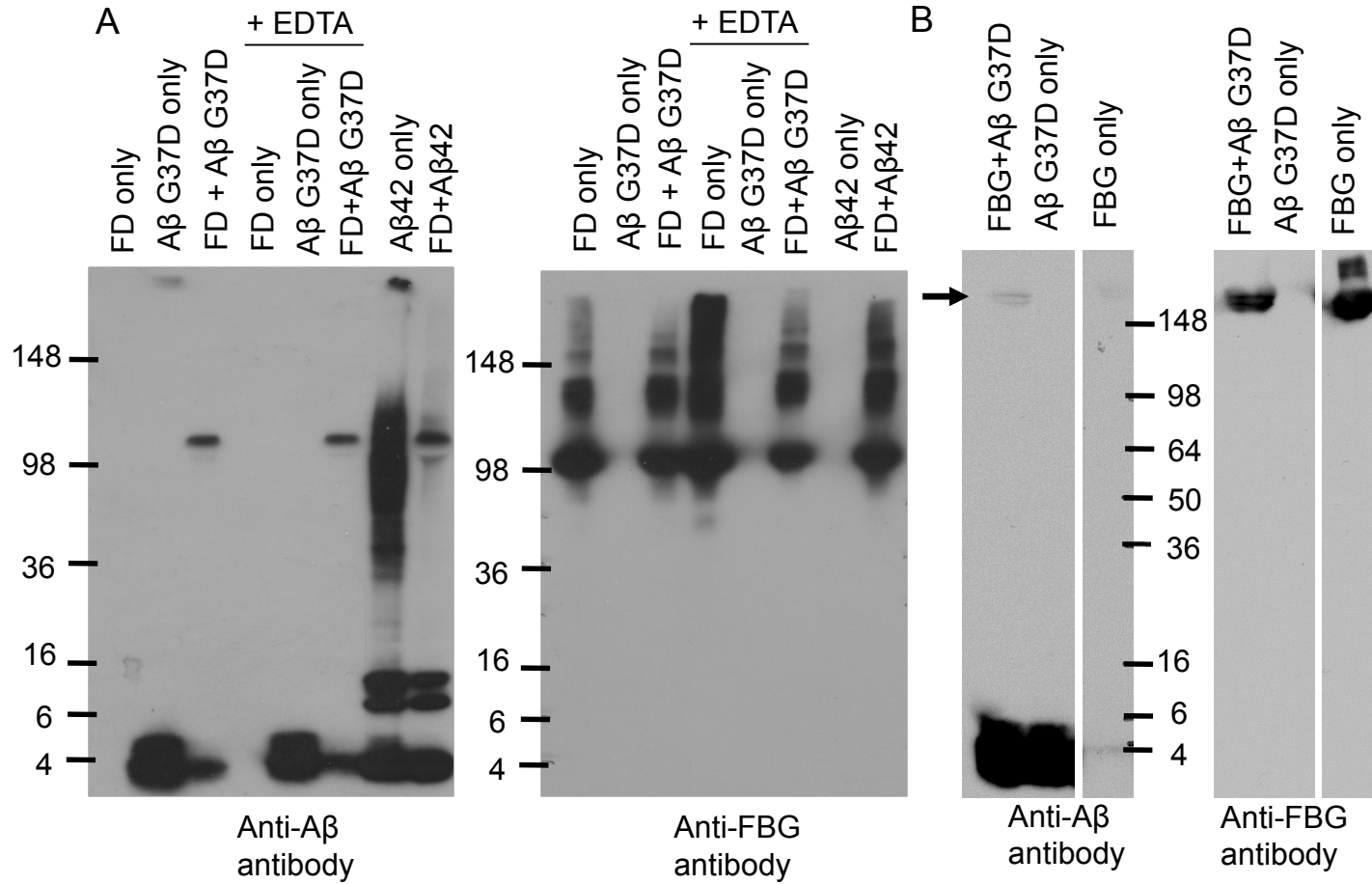
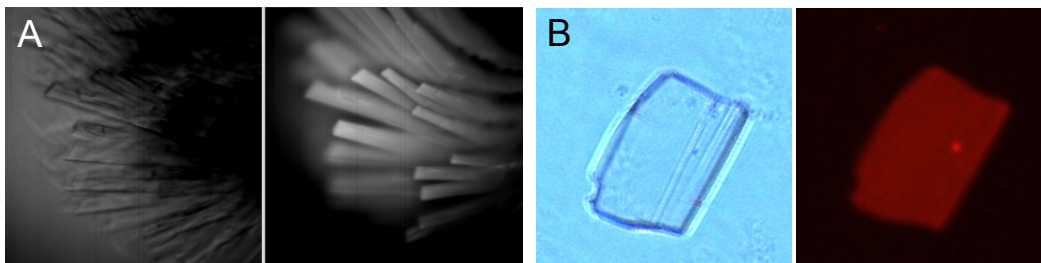


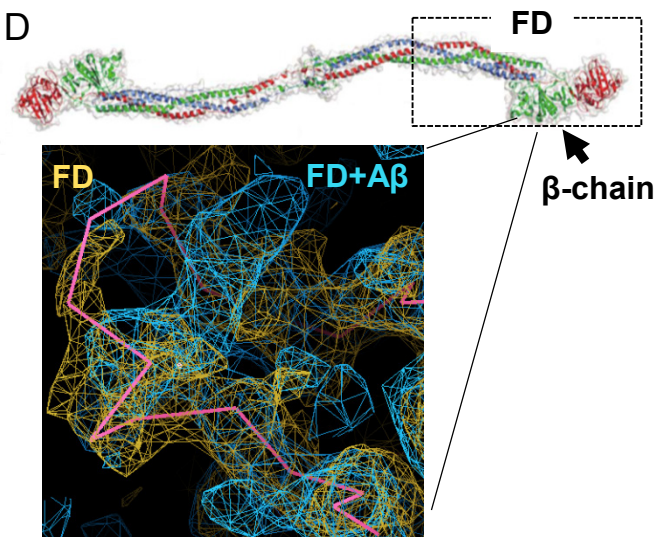
# Figure 5



**C**

	a	b	c	$\alpha$	$\beta$	$\gamma$
1FZA	107.72	48.08	167.56	90	105.70	90
Fragment D	100.40	45.99	163.57	90	104.54	90
Fragment D + A $\beta$ 42	100.37	45.81	168.45	90	105.74	90

**D**



**E**

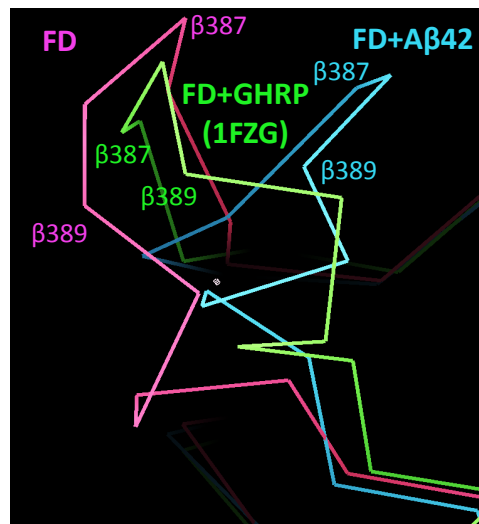
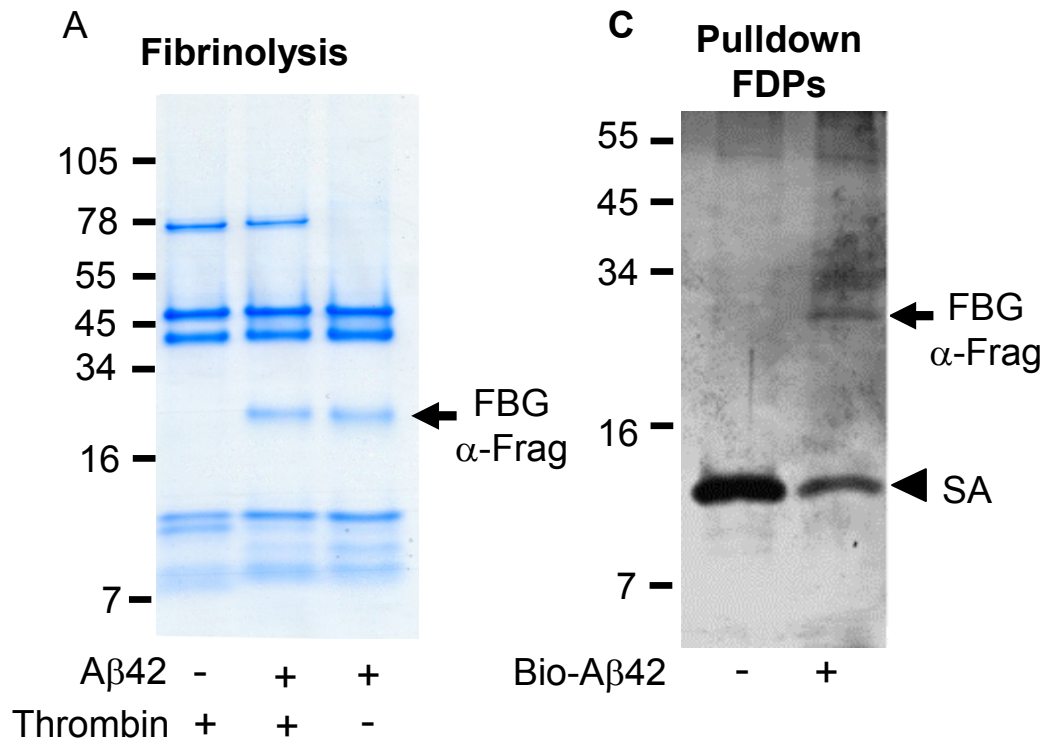


# Figure 6



**B**

	<b>M240</b>	<b>FBG α-chain</b>			
231	ALTDMPQMR <b>M ELERPGGNEI</b>	<b>TRGGSTSYGT</b>	<b>GSETESPRNP</b>	<b>SSAGSWNSGS</b>	
281	<b>SGPGSTGNRN</b>	PGSSGTGGTA	TWKPGSSGPG	STGSWNSGSS	GTGSTGNQNP
331	GSPRPGSTGT	WNPSSSERGS	AGHWTSESSV	SGSTGQWHSES	GSFRPDSPG
381	SGNARPNNPD	WGTFEEVSGN	VSPGTR <b>REYH</b>	<b>TEKLVTSKGD</b>	<b>KELRTGKEKV</b>

**K421**



**blood**<sup>®</sup>

Prepublished online July 7, 2016;  
doi:10.1182/blood-2016-03-705228

## **Biochemical and structural analysis of the interaction between $\beta$ -amyloid and fibrinogen**

Daria Zamolodchikov, Hanna E. Berk-Rauch, Deena A. Oren, Daniel S. Stor, Pradeep K. Singh, Masanori Kawasaki, Kazuyoshi Aso, Sidney Strickland and Hyung Jin Ahn

---

Information about reproducing this article in parts or in its entirety may be found online at:  
[http://www.bloodjournal.org/site/misc/rights.xhtml#repub\\_requests](http://www.bloodjournal.org/site/misc/rights.xhtml#repub_requests)

Information about ordering reprints may be found online at:  
<http://www.bloodjournal.org/site/misc/rights.xhtml#reprints>

Information about subscriptions and ASH membership may be found online at:  
<http://www.bloodjournal.org/site/subscriptions/index.xhtml>

---

Advance online articles have been peer reviewed and accepted for publication but have not yet appeared in the paper journal (edited, typeset versions may be posted when available prior to final publication). Advance online articles are citable and establish publication priority; they are indexed by PubMed from initial publication. Citations to Advance online articles must include digital object identifier (DOIs) and date of initial publication.